International Journal of Electrical, Electronic and Communication Sciences
ISSN: 2517-9438
Vol:5, No:5, 2011

Integration of Fixed and Variable Speed Wind Generator Dynamics with Multimachine AC Systems

A.H.M.A.Rahim

Abstract**—**The impact of fixed speed squirrel cage type as well as variable speed doubly fed induction generators (DFIG) on dynamic performance of a multimachine power system has been investigated. Detailed models of the various components have been presented and the integration of asynchronous and synchronous generators has been carried out through a rotor angle based transform. Simulation studies carried out considering the conventional dynamic model of squirrel cage asynchronous generators show that integration, as such, could degrade to the AC system performance transiently. This article proposes a frequency or power controller which can effectively control the transients and restore normal operation of fixed speed induction generator quickly. Comparison of simulation results between classical cage and doubly-fed induction generators indicate that the doubly fed induction machine is more adaptable to multimachine AC system. Frequency controller installed in the DFIG system can also improve its transient profile.

Keywords**—**Doubly-fed generator, Induction generator, Multimachine system modeling, Wind energy systems

I. Introduction

IN the early stage of wind power development, most wind farms were equipped with fixed-speed wind turbines and cage type induction generators. Since such generators can only operate at a constant speed, the power efficiency is fairly low for most wind speeds [1]. To improve their efficiency, wind generators adopt a variable speed operation in one of two ways: direct AC to AC frequency converters, such as the cycloconverters [2, 3], or using voltage controlled inverters which convert power at varying frequencies at the variable-speed generator to DC, and then use some form of power electronics to convert the DC power back to AC at a fixed frequency appropriate for the grid connection [4, 5]. As far as variable-speed generation is concerned, it is necessary to produce constant-frequency electric power from a variable-speed source [6-8]. Synchronous generator can also be used for this purpose provided that a static frequency converter is used to interface the machine with the grid.

An alternative approach involves using a wound-rotor induction generator fed with variable frequency rotor voltage. This allows fixed-frequency electric power to be extracted from the generator stator [9]. Consequently, the use of doubly fed induction machines is receiving increasing attention for wind generation purposes [10-12]. In the DFIG concept, the induction generator is grid-connected at the stator terminals, but the rotor terminals are connected to the grid via a partial-load variable frequency AC-DC-AC voltage source converter (VSC) and a transformer. The VSC only needs to handle a fraction (25-30%) of the total power to achieve full control of the generator. Compared to the fixed-speed wind turbine generator, the variable speed wind turbine (VSWT) with DFIG can provide decoupled control of active and reactive power of the generator, more efficient energy production, improved power quality, and improved dynamic performance during power system disturbances such as network voltage sags and short circuits. Compared to the VSWT equipped with a synchronous generator, in which a full load VSC is connected directly between the generator stator and the grid, the VSC of the DFIG is smaller in size and, therefore, is cheaper.Though DFIG has advantages over the other variable speed generator systems and future growth is directed this way, large number of classical induction generators are still in operation. Possible implications of connection of these cage machines to existing AC systems need careful study. The studies reported for multi-machine asynchronous-synchronous machines often refer to various types of commercial power system dynamic simulation packages [13-16]. These, generally, consider the asynchronous generator as a device which merely injects real power drawing reactive power which may not adequately represent their electrical behavior under transient conditions. This article develops detailed dynamic models of fixed speed classical cage generators as well as more modern variable speed doubly fed machine and interconnects them with multimachine AC synchronous systems. System behavior is investigated for different contingencies and introduction of frequency controller is suggested for better transient performance.

A.H.M.A.Rahim is with the Department of Electrical Engineering, King Fahd University of Petroleum &Minerals, Dhahran, Saudi Arabia (email: ahrahim@kfupm.edu.sa)

II. Wind Generator Systems

Fig.1 shows the schematic of an AC power system having an in-feed from an asynchronous wind generation system. The wind system comprises of a horizontal axis wind turbine and a squirrel-cage induction generator which connects to the multimachine system through its transmission network. The schematic of the doubly fed induction generator (DFIG) system is shown in Fig.2. Similar to the classical induction generator, the DFIG is also driven by a horizontal axis wind turbine through its gear boxes. The difference in the generator systems is that in the DFIG the converters are located between the rotor terminals and the grid of the wound-rotor machine. The converters are protected through a *crow-bar* protection system for over voltages. The wind turbines are considered to

be equipped with speed regulating systems which can control their power input to the induction generators.

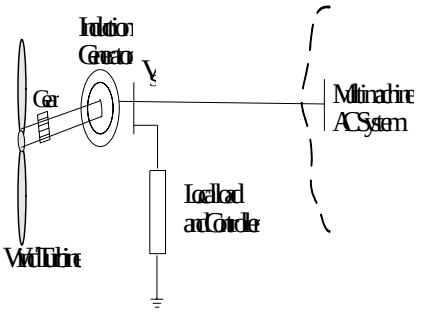

Fig.1 Variable speed cage induction generator in a power system

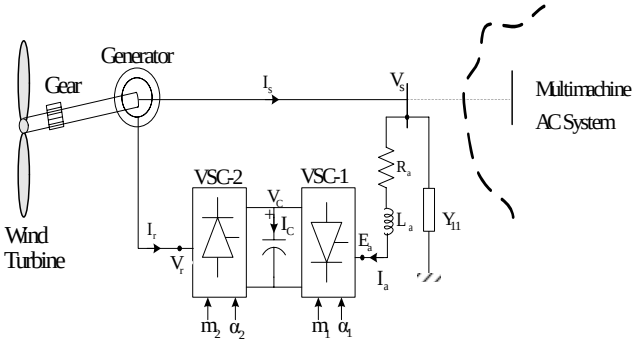

Fig.2 Doubly-fed induction generator connected to a power system

III. Component Models

Models for the various components of the two types of wind generation system including the induction and synchronous generators are presented in brief in the following sections.

A. *Wind Turbine Power Output*

The mechanical power output of a wind turbine is related to the wind speed V_ω by [17],

$$P_m = \frac{1}{2}\rho A C_p V_\omega^3 \tag{1}$$

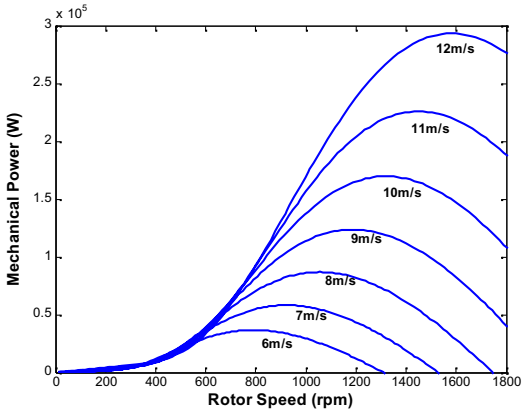

Fig. 3 Speed vs. power output characteristics of a wind turbine

Here, ρ is the air density and A is the swept area by the turbine blades. The power coefficient C_p is a function of both tip speed ratio (λ) and the blade pitch angle (β). The tip speed ratio which is the ratio of linear speed at the tip of blades to the speed of wind is expressed as,

$$\lambda = \frac{\omega_m R}{V_w} \tag{2}$$

where, R and ω_m are the radius and the mechanical angular velocity, respectively of the wind turbine rotor. Some typical plots of P_m for various wind speeds, and for zero blade pitch angle, are shown in Fig.3.

B. *Induction Generator*

The induction generator model is based on the flux-voltage–current relationships of the stator and rotor circuits. If both stator and rotor transients are included, dynamics of a simple machine can be expressed by a 4th order model in terms voltages and currents in the form,

$$\begin{aligned}
\dot{i}_{ds} &= a_{11}i_{ds} + a_{12}i_{qs} + a_{13}e'_d + a_{14}e'_q + b_{11}v_{ds} + b_{13}v_{dr} \\
\dot{i}_{qs} &= a_{21}i_{ds} + a_{22}i_{qs} + a_{23}e'_d + a_{24}e'_q + b_{22}v_{qs} + b_{24}v_{qr} \\
\dot{e}'_d &= a_{31}i_{ds} + a_{32}i_{qs} + a_{33}e'_d + a_{34}se'_q + b_{34}v_{qr} \\
\dot{e}'_q &= a_{41}i_{ds} + a_{42}i_{qs} + a_{43}se'_d + a_{44}e'_q + b_{42}v_{dr}
\end{aligned} \tag{3}$$

Here, i_{ds}, i_{qs}, v_{ds} and v_{qs} are the d-q components of stator current and voltage, respectively; e_d' and e_q' are the components of the internal voltage E' behind transient impedance Z' = R_s + j x' of the induction machine. The coefficients a_{11}, a_{12}, …..;b_{11}, b_{12}, ….., etc. depend on machine parameters. If the stator transients are neglected, the first two dynamic equations will be replaced by the following algebraic ones in terms of the stator voltage, current, and internal voltages,

$$\begin{aligned}
v_{ds} &= -R_s i_{ds} + x' i_{qs} + e'_d \\
v_{qs} &= -R_s i_{qs} - x' i_{ds} + e'_q
\end{aligned} \tag{4}$$

The state equations depend on the slip of the machine expressed as,

$$s = \frac{\omega_0 - \omega_R}{\omega_0} \tag{5}$$

A two-mass model for the turbine–generator system is adopted as higher inertia wind turbine rotor is connected to the low inertia IG rotor with a relatively soft shaft. The dynamic equations of the two-mass representation are expressed as,

$$2H_t \frac{d\omega_t}{dt} = P_m - K_s\theta_s - D_t\Delta\omega_t \tag{6}$$

$$2H_g \frac{d\omega_r}{dt} = K_s\theta_s - P_e - D_g\Delta\omega_r \tag{7}$$

$$\frac{d\theta_s}{dt} = \omega_b(\omega_t - \omega_r) \tag{8}$$

Here, θ_s is the shaft torsion angle, K_s is the shaft stiffness, and D_t and D_g are the damping coefficients of turbine and generator respectively. The subscript *t*, *g* and *s* refer to the turbine and generator and shaft quantities respectively; P_e is the generator output power given as,

$$P_e = x_m i_{qr} i_{ds} - x_m i_{dr} i_{qs} \tag{9}$$

Though a grid connected machine can derive excitation from the AC system, additional excitation, if needed, is provided by static capacitor connected at the generator terminal. This can be used for power factor correction purposes also.

C. Induction Generator Speed Regulator

For automatic control of speed of the asynchronous generators they need to be equipped with mechanical or electromechanical devices so as to relate the power input and output of the generator. For a constant setting of the speed changer the static increase in generator output is directly proportional to static frequency droop (1/R). After the primary control function, which brings the system to an equilibrium state with a permanent frequency error, a secondary control is needed which eventually establishes nominal rotational speed by eliminating the static speed error. The device which performs this action is the speed or frequency error signal integrator as shown in Fig.4 [18].

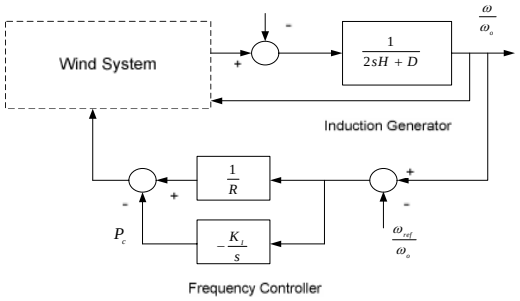

Fig.4 The frequency controller configuration of an induction generator

The frequency controller, which is similar to a PI controller, can be described by the equations,

$$\begin{aligned} \dot{P}_c &= -\frac{K_I}{\omega_o}\frac{\Delta\omega_R}{\omega_o} \\ \Delta P_m &= \Delta P_c - \frac{1}{R}\frac{\Delta\omega_R}{\omega_o} \end{aligned} \tag{10}$$

D. The Doubly Fed Induction Generator

The voltage-current-flux relationships of a doubly fed induction generator are the same as in the classical squirrel machine given in (4) except that the rotor voltages [v_{dr} v_{qr}] along the d-q axes are controlled by a converter controlled circuit in the feedback path. The electronic circuit in the rotor circuit of the DFIG system given in Fig. 2 is an integral and vital component of the generator and has to be adequately modeled. The additional equations arising out of the stator side converter transformer circuit are,

$$\frac{d}{dt}\begin{bmatrix} i_{ad} \\ i_{aq} \end{bmatrix} = \frac{\omega_o}{L_a}\begin{bmatrix} -R_a & L_a \\ -L_a & -R_a \end{bmatrix}\begin{bmatrix} i_{da} \\ i_{qa} \end{bmatrix} + \frac{\omega_o}{L_a}\begin{bmatrix} v_{ds} - e_{ad} \\ v_{qs} - e_{aq} \end{bmatrix} \tag{11}$$

In the above,

$$\begin{aligned} e_{ad} &= m_1 V_c \cos\alpha_1 \\ e_{aq} &= m_1 V_c \sin\alpha_1 \end{aligned} \tag{12}$$

The factor m_1 is the modulation index of the voltage source converter VSC-1, and α_1 is the phase difference of the converter AC voltage E_a with respect to the system reference. V_c is the voltage of the DC coupling capacitor between the stator side voltage source converter VSC-1 and rotor side converter VSC-2. The components of the rotor voltage are written as,

$$\begin{aligned} v_{dr} &= m_2 V_c \cos\alpha_2 \\ v_{qr} &= m_2 V_c \sin\alpha_2 \end{aligned} \tag{13}$$

α_2 and m_2 refer to the phase and modulation index of rotor side converter VSC-2. Considering the converters to be lossless, and equating the powers at the two sides of each converter one gets, it can be shown that the DC coupling capacitor satisfies the differential equation,

$$\frac{dV_c}{dt} = \frac{1}{C}[m_1\cos\alpha_1 i_{da} + m_1\sin\alpha_1 i_{qa} + m_2\cos\alpha_2 i_{dr} + m_2\sin\alpha_2 i_{qr}] \tag{14}$$

E. Synchronous Generator

Neglecting the stator transients, the synchronous generator is represented through a 5th order model [19],

$$\begin{aligned} \dot{e}'_q &= \frac{1}{T'_{do}}\left[E_{fd} - e'_q - (x_d - x'_d) i_{ds}\right] \\ \dot{e}'_d &= \frac{1}{T'_{qo}}\left[-e'_d + (x_q - x'_q) i_{qs}\right] \\ \dot{\omega} &= \frac{1}{2H}\left[P_m - P_e - P_D\right] \\ \dot{\delta} &= \omega_0 \Delta\omega \\ \dot{E}_{fd} &= \frac{1}{T_A}\left[K_A(V_{ref} - V_t) - E_{fd}\right] \end{aligned} \tag{15}$$

Here, the states $[e'_d \; e'_q \; \delta \; \omega \; E_{fd}]$ are generator d-q internal voltages, rotor angle, speed and the field voltage, respectively. The terminal voltage along d-q axes, and torque output equations are,

$$\begin{aligned} v_{ds} &= -r_s i_{ds} + x'_q i_{qs} + e'_d \\ v_{qs} &= -r_s i_{qs} - x'_d i_{ds} + e'_q \\ P_e &= e'_d i_{ds} + e'_q i_{qs} + (x'_q - x'_d) i_{ds} i_{qs} \end{aligned} \tag{16}$$

IV. MULTIMACHINE SYSTEM MODEL

In multimachine AC system modeling the voltages and currents of the synchronous machines in their own (d-q) frames are related to the network (D-Q) frame though,

$$[F]_{DQ} = [T][F]_{dq} \tag{17}$$

The transformation matrix T is,

$$T = dig[e^{j(\delta-\pi/2)}] = diag[rot(\delta_1), rot(\delta_2), ..., rot(\delta_G)] \tag{18}$$

Here,

$$rot(\delta) = \begin{bmatrix} \sin\delta & \cos\delta \\ -\cos\delta & \sin\delta \end{bmatrix}$$

The phasor relationships between network frame (D-Q) and machine frame (d-q) quantities are shown in Fig.5(a). The induction generator equations can be written either in the network frame or in terms of machine frame. If the d-axis of the induction generator is considered to be aligned with its terminal voltage, definition of a corresponding induction generator rotor angle given by,

$$\delta_{ig} = \pi/2 + \arg(V_{ig}) \tag{19}$$

is compatible with the general transformation matrix given in (17). The phasor diagram representation is given in Fig.5 (b). Nomikos [20] in his work on multimachine systems considered the induction machine to be aligned with network D-Q frame with δig=0. Under steady state conditions, the terminal voltage of the induction machine is phase displaced from the D-Q frame, which is normally the frame of the reference machine. This concept of induction machine angle was considered in [18] also. In this analysis, we consider δig to remain constant at the initial value.

Representing all the loads in the power system by constant impedances, the currents injected by the sources can be expressed in terms of the node voltages through the reduced node admittance matrix Y_{red} by,

$$I_{Bus} = Y_{red} V_{Bus} \tag{20}$$

Using (17) the above equation can be expressed along the machine d-q components as,

$$I_{dq} = T^{-1} Y_{red} T V_{dq} \tag{21}$$

A generalized expression for the stator current-voltage relationships of the induction and synchronous generators, given in (4) and (16), can be written in the form,

$$V_{dq} = [Z] I_{dq} + E'_{dq} \tag{22}$$

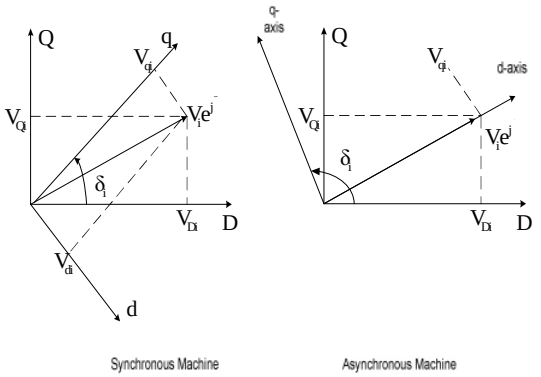

Fig. 5 Graphical representation of the relation between network (D-Q) and machine (d-q) reference frames of synchronous and asynchronous machines

Substituting (21) into (22), the non-state currents of the induction and synchronous generators are finally expressed in terms of the state variables as,

$$I_{dq} = [1 - Y_m Z]^{-1} Y_m E'_{dq} \tag{23}$$

These are substituted in the differential equations for the induction and synchronous generators (3) and (15) to give a closed form state representation. The complete state model for the power system contains the asynchronous machine (cage or doubly-fed) including its frequency controller and the synchronous AC system and is expressed in the form,

$$\dot{x} = f(x, u) \tag{24}$$

V. SIMULATION RESULTS: WITH CAGE-GENERATOR

A multimachine power system shown in Fig. 6 is simulated for this study with induction generator in-feed at bus 4. It is assumed that 68 MW is being supplied by the wind farm which has 50 generators each with a capacity of 2MW. This is approximately 26% of total system generation. The system data is given in the Appendix. Typically, in steady state load flow analysis the induction generator is represented as a PQ bus [21]. However, in this study it was considered to be a PV bus having the provision of an additional excitation capacitor at the generator terminal. The capacitance at the bus can be adjusted so that the induction generator system operates almost under unity power factor condition [22]. The slip of the machine is established from the static steady state model of the induction generator and the corresponding reactive power absorbed by the generator is calculated.

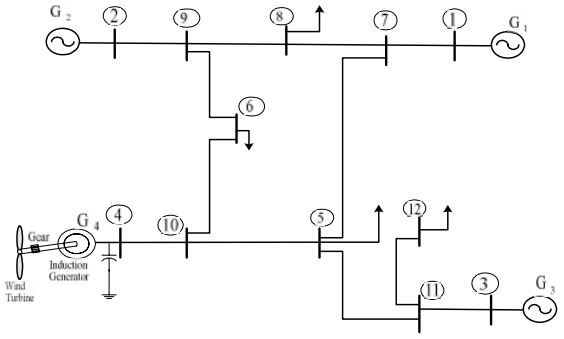

Fig. 6 Multimachine system configuration including asynchronous machine

The transient behavior of the system was investigated for torque pulse as well as three-phase fault conditions considering two modeling scenarios. These are, (a) with the proposed frequency or power controller, and (b) without the controller.

Figs.7-11 show the induction generator transient response for a short 50% input torque pulse for 0.5s duration. This small disturbance is introduced to study the nature of transients which may arise in the integrated system. The variation of the machine slip following the disturbance in Fig.7 shows that the system is slightly oscillatory without any control. Also, it shows a slip error which decays extremely slowly. The corresponding plots for the magnitude and phase angles of the generator terminal voltage are shown in Figs. 8 and 9 (labeled 'no control'). While the magnitude of the terminal voltage shown in Fig.8 behaves quite normally, an interesting phenomenon is observed in the phase angle of the generator terminal voltage plotted in Fig. 9. It can be seen that the phase angle continues to grow in a cyclic manner. Since the phase angle shift phenomenon occurs in current phasors in a similar manner, it is not reflected in power output of the machine. However, since the input currents from all the generators to the network are interrelated the phase angle change in one will affect the others.

The drift in this phase angle behavior is the result of the error in slip from its steady value. Referring to Fig.7, the magnitude of the slip error at around t=15s is approximately 0.0016 and the period of phase angle rotation from Fig. 9 is about 10s, which can be related as,

$$T = \frac{2\pi}{|\Delta s|\omega_0} \qquad (25)$$

Figs. 10 and 11 further illustrate the phenomenon of phase angle drift from the record of stator currents of the induction generator. From Fig.11 it can be observed that while the magnitude of the stator current without any control settles down quite quickly, the d-q components of stator current (I_d, I_q) continue to oscillate at the slip frequency determined by (25).

The phase angle drift can be rectified by using a frequency or power controller in the induction generator system which has been presented in section IIIC. The frequency controller restores the system frequency to the pre-disturbance value. Figs. 7-9 (solid lines) show the variation of slip, magnitude and phase of terminal voltage, respectively when the frequency controller is installed. It can be seen that the frequency controller eliminates the slip error very fast. The drift of the phase angle of voltage and current phasors has been stopped in about 2 seconds as shown in Figs. 9 and 11 (solid line).

Figs. 12 and 13 show the change in induction generator slip (Δs) and change in phase angle of the terminal voltage following a 0.5s three-phase fault near the generator terminal. Steady slip error of about 0.004 results in the cyclic oscillation of the terminal voltage phase angle having a period of approximately 4s. The inclusion of frequency controller in this case also restores normal operation quickly as are exhibited in Figs 12 and 13 (solid lines).

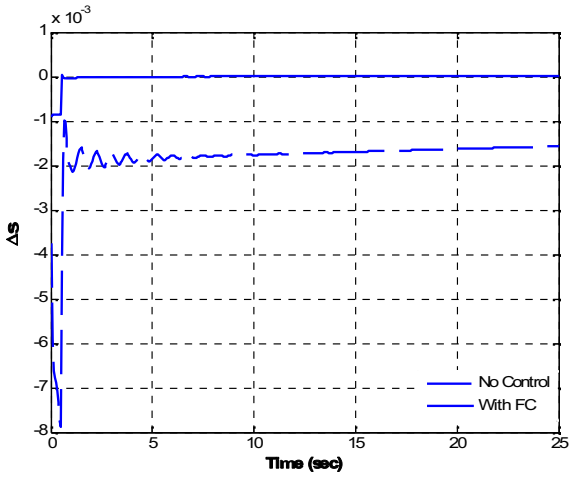

Fig.7 Change in induction generator slip following a 50% input torque pulse with, a) No control and, b) proposed frequency controller

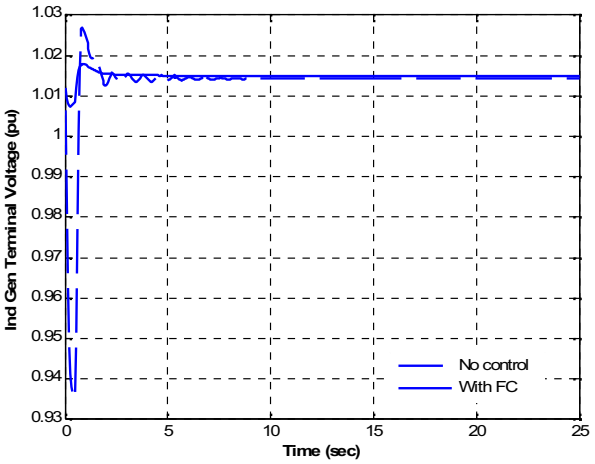

Fig. 8 Magnitude of induction generator terminal voltage variation corresponding to Fig.7

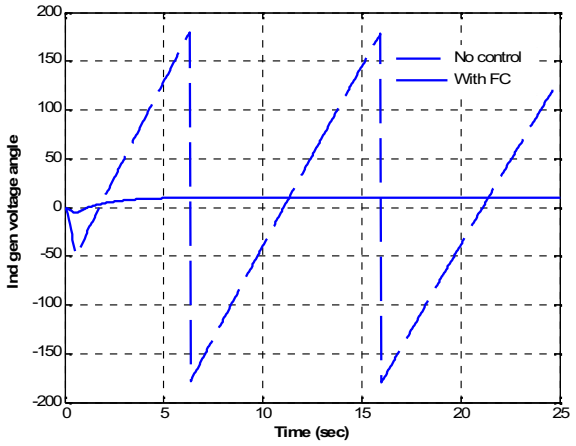

Fig. 9 Induction generator terminal voltage phase angle variation corresponding to Fig.7

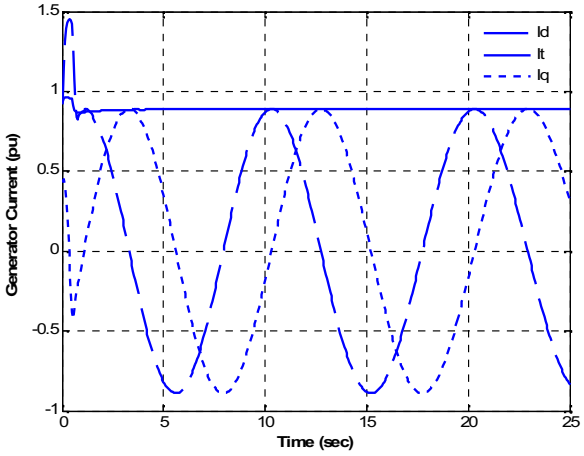

Fig. 10 Induction generator stator current following a 50% input toque pulse without any control; responses are with, a) d-axis component of stator current Id, b) q-axis component of stator current Iq and, c) the magnitude of stator current It

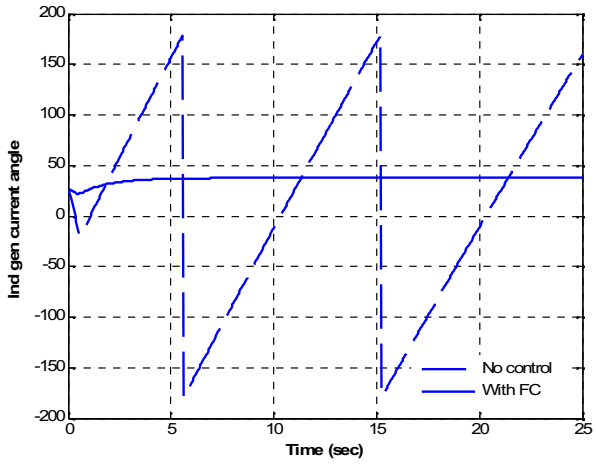

Fig.11 Induction generator stator current phase angle variations considering, a) No control, b) with frequency controller

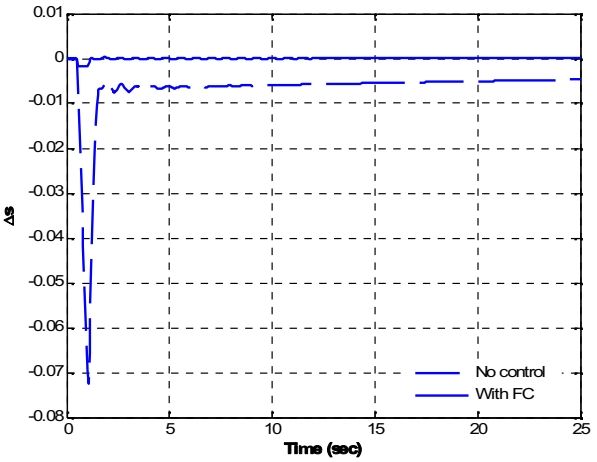

Fig.12 Slip variation of induction generator following a 0.5s three-phase fault considering, a) No control, b) with frequency controller

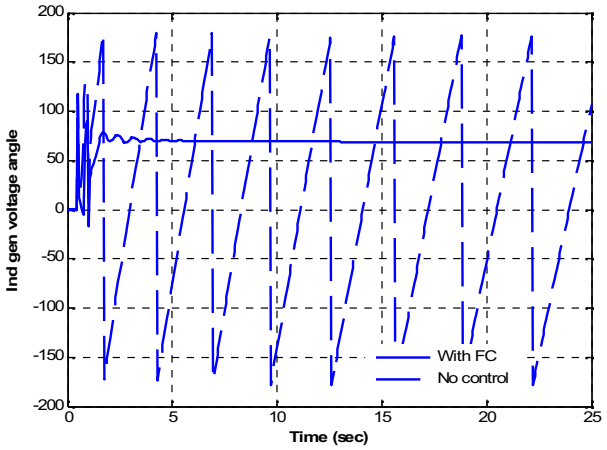

Fig.13 Comparison of generator terminal voltage phase angles corresponding to Fig.12

VI. SIMULATON RESULTS: DOULY-FED GENERATOR

The cage induction machine at bus 4 in Fig. 6 was replaced with a doubly fed induction generator. For the same loading condition as in the cage generator, a three-phase fault of 0.5s duration was simulated on bus 10. The change of slip, the terminal voltage magnitude and voltage phase angle are plotted in Figs. 14-16, respectively. Responses are shown for the 2 scenarios considered earlier, the conventional model without a frequency controller and the other one including a frequency controller. The frequency controller eliminates the error between the nominal and actual speeds and normal operating conditions are restored in about 3s. These are exhibited by solid line in all the three figures. Contrary to the cage induction generator case, the angles of the voltage and current phasors do not go through these periodic growths. This is because; the doubly fed machine itself is controlled for real and reactive power internally through its converters. Hence, dynamic integration of such devices to multimachine AC system is simpler.

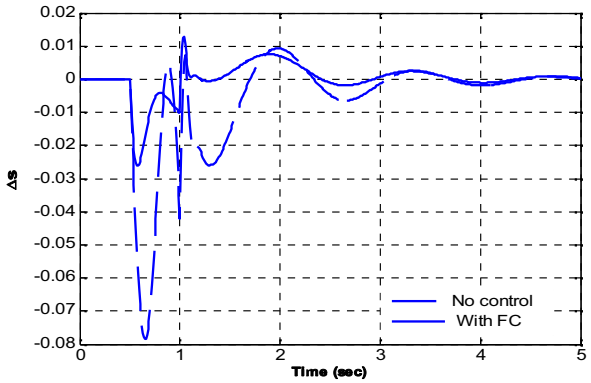

Fig. 14 DFIG slip variation following a three-phase 0.5s fault with and without proposed frequency controller

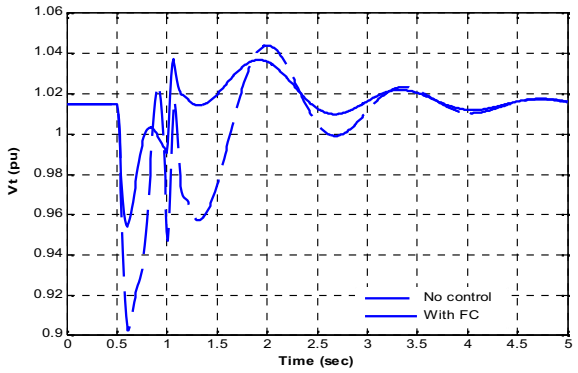

Fig.15 Variation of DFIG terminal voltage magnitude for the disturbance condition corresponding to Fig. 14

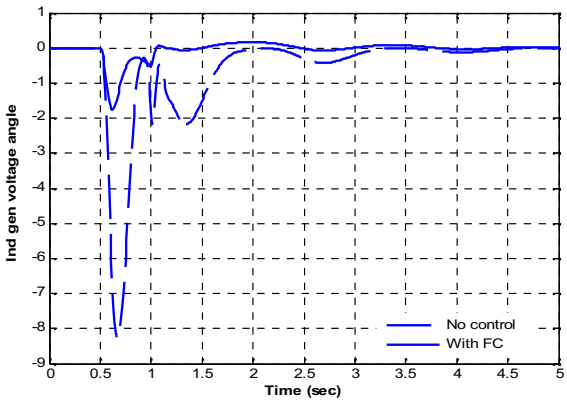

Fig.16 Phase angle of the DFIG terminal voltage phasor corresponding to Fig.14

VI. Conclusions

A comparative study of the dynamic behavior of fixed speed classical cage generator and variable speed doubly fed wound-rotor induction generator systems when connected to a multimachine system has been carried out. The variables of the asynchronous and synchronous machines in the multimachine system are converted through a rotor angle dependent transform. In the absence of adequate frequency control, the slip error of fixed speed cage machine can be a potential source of electrical transients to the synchronous system affecting its power quality. A frequency or power controller in the asynchronous machine corrects the steady slip error controlling the cyclic growth of the voltage and current phase angles. Results indicate that the problem of growing phase angle and resultant transient in machine currents do not arise in doubly fed generator modeling. This is because the converters in the rotor circuit of DFIG internally control the real and reactive power to a certain degree. Incorporation of a frequency controller in the doubly-fed system, however, further improves the dynamic profile.

Acknowledgements

This work was part of KFUPM sponsored research grant RG1006-1& RG1006-2. The author wishes to acknowledge the facilities provided by the King Fahd University of Petroleum & Minerals.

Nomenclature

d-q	Direct and quadrature axes
R_s	Induction generator stator resistance
x'	IG transient reactance
x_d , x_q'	Synchronous generator transient reactance
i_{ds}, i_{qs}	d-q axes stator current
i_{dr}, i_{qr}	d-q axes rotor current
v_{ds}, v_{qs}	d-q axes stator voltage
v_{dr}, v_{qr}	d-q axes rotor voltage
e'_d , e'_q	d-q axes internal voltages of generator
s	slip of induction generator
E_{fd}	Synchronous generator field voltage
V_{tr}	Reference terminal voltage
K_A, T_A	Excitation system gain and time constant
ω_R, ω_o	IG rotor speed, base angular speed
H, D	Inertia constant, damping coefficient of generator
P_D	Damping power
V_c	Coupling capacitor voltage
ω	Angular speed of synchronous generator

Appendix

Parameters of the Multimachine System:

Table I
Generation and Load Data

	Generation		**Load**	
Bus #	P_g MW	Q_g MVAR	P_L MW	Q_L MVAR
1	37.55	23.94		
2	105	16.107		
3	50	19.603		
4	68	-		
5			77.5	30
6			52.5	25
8			72.5	27
12			48.75	15

TABLE II
LINE DATA IN 100 MVA BASE

From bus	To bus	R_{line} (pu)	X_{line} (pu)	B/2 (pu)
1	7	0	0.05	0
2	9	0	0.05	0
4	10	0.08	0.4	0
3	11	0	0.05	0
11	12	0.018	0.1167	0.0175
11	5	0.009	0.10	0.035
5	10	0.009	0.1167	0.035
10	6	0.009	0.135	0.035
6	9	0.009	0.1075	0.035
9	8	0.009	0.11	0.049
8	7	0	0.1333	0.035
7	5	0.009	0.1333	0.035

REFERENCES

[1] Y. Lei , A. Mullane, G. Lightbody, and R. Yacamini (2006), " Modeling of the wind turbine with a doubly fed induction generator for grid integration studies", IEEE Trans. Energy Conversion, Vol 21, pp.257-264, 2006
[2] M. Machmoum, R. Doeuff, F. Sargos, "Steady state analysis of a doubly fed asynchronous machine supplied by a current controlled cycloconverter in the rotor", Proc. Inst. Elect. Eng. B Vol 139, pp.114–122, 1992
[3] P. Holmes, N. Elsonbaty, "Cycloconverter excited divided winding doubly fed machine as a wind power converter", Proc. Inst. Elect. Eng. B Vol 131, pp. 61–69, 1984
[4] P. Carlin, A. Laxson, E. Muljadi, "The history and State of the art of variable-speed wind turbine technology", National Renewable Energy Lab., Tech. Rep, NREL/TP-500-28 607, 2001
[5] A. Neris, N. Vovos, G. Giannakopaulos, "A variable speed wind energy conversion scheme for connection to weak ac systems", IEEE Trans. Energy Conversion, Vol 14, pp.122–127, 1999
[6] A. Tapia, G. Tapia, J. Ostolaza, J. Sáenz, "Modeling and control of a wind turbine driven doubly fed induction generator", IEEE Trans. Energy Conversion , Vol 18:, pp.194-200, 2003
[7] D. Leith, W. Leithead, "Appropriate realization of gain-scheduled controllers with application to wind turbine regulation", Int. Journal of Control, Vol 65, pp. 223–248, 1996
[8] B. Ooi, R. David, "Induction-generator/synchronous-condenser system for wind-turbine power.", Proc. Inst. Elect. Eng., Vol 126, pp.69–74, 1979
[9] J.G. Sloothweg, H. Polinder, W. Kling, "Dynamic modeling of a wind turbine with doubly fed induction generator", Proc. IEEE Power Eng. Soc. Summer Meeting, Vancouver, 2001
[10] R. Spee, S. Bhowmik, J. Enslin, " Novel control strategies for variable-speed doubly fed wind power generation systems", Renewable Energy Vol 6, pp.907–915, 1995
[11] M. Nunes, J.M. Pecas Lopes, H. Zurn, U. Bezerra, R. Almeida , "Influence of the variable-speed wind generators in transient stability margin of the conventional generators integrated in electrical grids" , IEEE Trans. Energy Conversion, Vol 19, pp.692-701, 2004
[12] J. Morren , S. de Haan, "Ridethrough of wind turbines with doubly-fed induction generator during voltage dip", IEEE Trans. Energy Conversion, Vol 20, pp.435-441, 2005
[13] J. Slootweg, Wind power – modeling and impact on power system dynamics. Ph. D. Thesis: Delft Technical University, Netherlands, 2003
[14] S. Muyeen, R. Takahashi, M. Ali, T. Murata, J. Tamura , "Transient stability augmentation of power system including wind farms by using ECS", IEEE Trans on Power Systems, Vol 23:, pp.1179-1187, 2008
[15] C. Jauch , P. Sørensen, I. Norheim, C. Rasmussen, "Simulation of the impact of wind power on the transient fault behavior of the Nordic power system.", Electric Power Systems Research , Vol 77, pp. 135-144, 2007
[16] V. Vowles, C. Samarasinghe, M. Gibbard, G. Ancell, "Effect of wind generation on small-signal stability – A New Zealand example", IEEE Power & Energy Society General Meeting, pp.1-8., 2008
[17] A.H.M.A.Rahim and I.O.Habiballah, "DFIG Rotor Voltage Control for System Dynamic Performance Enhancement", Electric Power Systems Research, Vol 81, pp. 503-509, 2011
[18] G.S. Stavrakasis, G.N. Kariniotakis, "A general simulation algorithm for the accurate assessment of isolated diesel-wind turbines system interaction. Part I: A general multimachine power system model", IEEE Trans. Energy Conversion, Vol 10, pp.577-583, 1995
[19] P. Kundur, Power System Stability and Control. EPRI Power System Engineering Series, 1994
[20] B.M.Nomikos and C.D. Vournos, "Evaluation of motor effects on the electromechanical oscillations of multimachine systems", 2003 IEEE Power Tech. Conference, Bologna, Italy, June 2003
[21] E. Feijoo, J. Cidras, "Modeling of wind farms in the load flow analysis", IEEE Trans on Power Systems, Vol. 15, pp.110-115, 2000
[22] V. Akhmatov, Induction Generators for Wind Power. Multi-Science Publishing Company Ltd, 2005